PERGAMON

Quaternary Science Reviews 21 (2002) 1643–1660

QSR

Modelling Late Cenozoic isostatic elevation changes in the Barents Sea and their implications for oceanic and climatic regimes: preliminary results

Faisal A. Butt[a,*], Helge Drange[b], Anders Elverhøi[a], Odd Helge Otterå[b], Anders Solheim[c]

[a] *Department of Geology, University of Oslo, P.O. Box 1047, N-0316 Oslo, Norway*
[b] *Nansen Environmental and Remote Sensing Center, Edv. Griegsv. 3A, N-5059 Bergen, Norway*
[c] *Norwegian Geotechnical Institute, P.O. Box 3930 Ullevål Stadion, N-0806 Oslo, Norway*

Received 5 April 2001; accepted 12 March 2002

Abstract

Late Cenozoic isostatic changes in the elevation of the Barents Sea are simulated using a numerical model. Isopach maps of the deposits off present-day Bear Island and Storfjorden troughs made earlier are used to calculate the thickness of sediment cover removed from the respective drainages basins at various time intervals during the last 2.3 Ma. Results indicate that Barents Sea was subaerially exposed at 2.3 Ma and major parts of it became submarine after 1 Ma. Barents Sea today receives around 40% of the warm and saline North Atlantic waters flowing into the Scotland–Greenland Ridge and about half of the Atlantic water entering the Arctic Ocean. It thus has an important role to play in the present-day ocean circulation pattern in the Polar North Atlantic region and water-mass transformations that take place in the Greenland–Iceland–Norwegian Sea and the Arctic Ocean. The effects of an uplifted Barents Sea on the oceanic regime and the Arctic sea-ice cover under the present-day forcings fields are studied using the Miami Isopycnic Coordinate Ocean Model. Preliminary results indicate that a subaerial Barents Sea causes an increased input of warm Atlantic waters into the Arctic Ocean through the Fram Strait which results in warming of the Atlantic water masses in the Arctic Ocean, followed by a reduction in the sea-ice cover. The obtained findings can be used to explain the apparent discrepancy in the late Cenozoic record of the sub-Arctic and Arctic regions whereby Fennoscandia, Iceland and Greenland are envisaged to have been covered by major ice sheets during late Pliocene whereas high Arctic areas such as Svalbard and NE Greenland were apparently free of any major ice.

1. Introduction

The present-day climate at high northern latitudes is regulated by the advection of warm North Atlantic waters into the Nordic Seas (Fig. 1) and the water-mass transformations that take place therein. The Barents Sea receives about 40% of these northward flowing waters and is thus an important part of the system (e.g., Simonsen and Haugan, 1996). It has since long been recognised that Barents Sea was subaerially exposed during pre-Quaternary times (e.g., Nansen, 1904, 1920). However, the transition from a continental region to an epicontinental shelf sea, in terms of oceanographic patterns and climatic evolution in the Polar North Atlantic, has received little attention.

In the present study, temporal shifts in the elevation of the Barents Sea are simulated using an isostatic model by Dimakis et al. (1998). The impact of an exposed Barents Shelf on the general ocean circulation and the thermodynamics in the region is then studied by a high latitude version (Drange, 1999) of the prognostic, three-dimensional ocean general circulation model (MICOM—Miami Isopycnic Coordinate Ocean Model, Bleck et al., 1992).

Such a study has become all the more relevant in view of the apparent discrepancies in the palaeoclimatic reconstructions of the Polar North Atlantic region during the Plio-Pleistocene. Major parts of Fennoscandia, Iceland and Greenland are envisaged to have been covered by large ice masses around 2.6 Ma (e.g., Jansen and Sjøholm, 1991) whereas

*Corresponding author. Present address: Department of Geography and Geology, University of the West Indies, Mona Campus, Kingston 7, Jamaica. Tel.: +1-876-927-2728; fax: +1-876-977-6029.
E-mail address: faisal.butt@uwimona.edu.jm (F.A. Butt).

0277-3791/02/$ - see front matter
PII: S0277-3791(02)00018-5

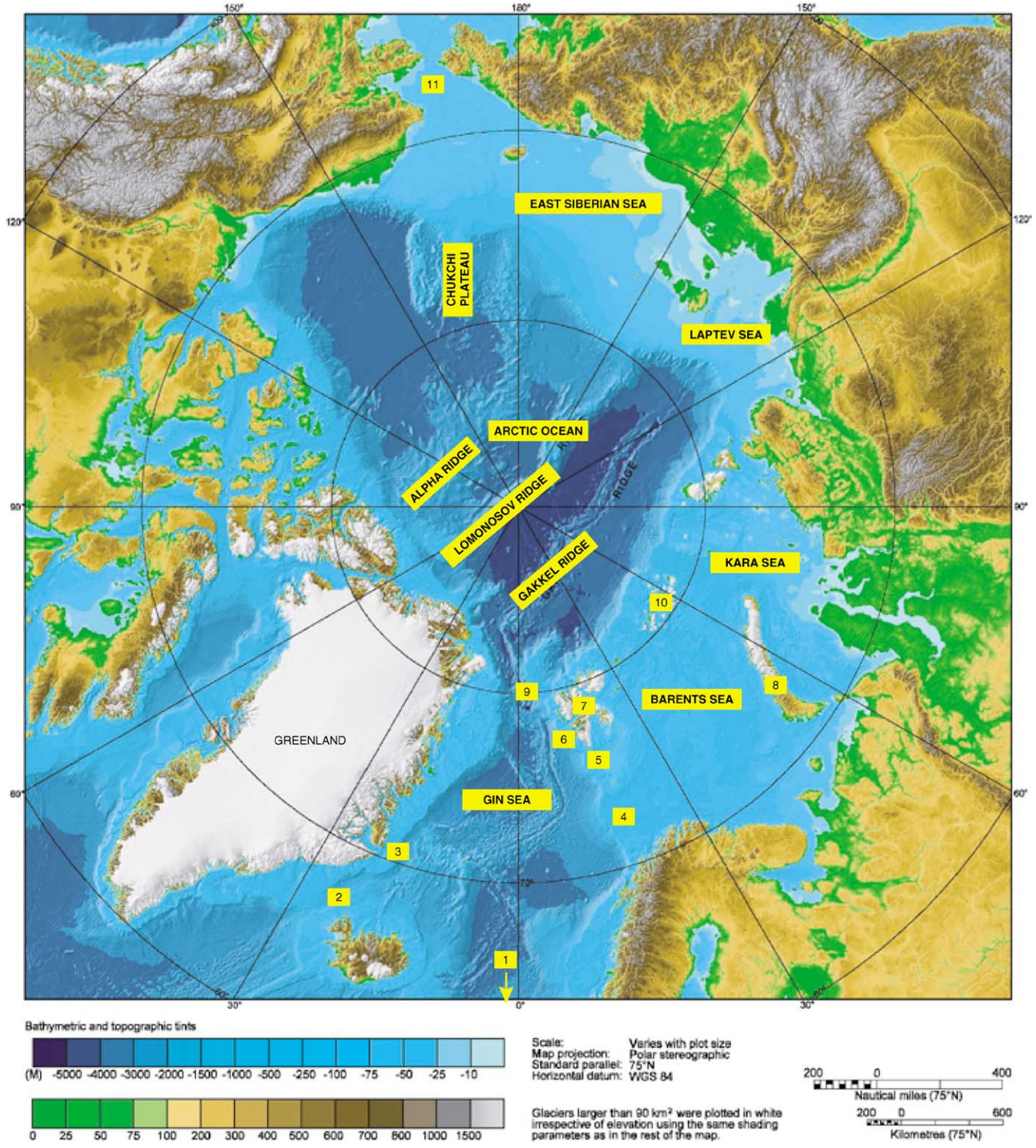

Fig. 1. Map over the Nordic Seas and the Arctic Ocean. 1, Færoe–Shetland Channel (to the south as indicated by the arrow); 2, Denmark Strait; 3, ODP Site 987 (approximate location); 4, Bear Island Trough; 5, Storfjorden Trough; 6, ODP Site 986 (approximate location); 7, Svalbard; 8, Novaya Zemlya; 9, Fram Strait; 10, Franz Josef Land; 11, Bering Strait (modified from IBCAO, 2000).

high-Arctic areas, such as NE Greenland and Svalbard, were probably free of any major ice accumulations at this time (e.g., Funder et al., 1985; Butt et al., 2000).

Probably, the most significant aspect of the ocean circulation pattern in high northern latitudes is the formation of deep waters in the Greenland–Iceland–Norwegian (GIN) Sea, and this convection is believed to

drive much of the global overturning cell in the ocean (Aagaard and Carmack, 1994). While the actual mechanism remains uncertain, it has been widely recognised that the magnitude and consistency of the North Atlantic Current (NAC), transporting warm and saline waters into the GIN Sea through the Færoe–Shetland Channel, is essential to the thermohaline balance and circulation patterns in the Polar North Atlantic (Hopkins, 1991). In moving from the Færoe–Shetland Channel to Svalbard, the temperature of NAC drops by 4–5°C (Johannessen, 1986). This drop in temperature results in the release of ~59 TW of heat to the atmosphere (Simonsen and Haugan, 1996) which is instrumental in moderating the present-day climate of Europe (Broecker et al., 1985).

Any perturbations in North Atlantic forcing are likely to affect the thermohaline circulation and consequently, the climate in the region. A weakening of NAC is likely to lead to cooling and a southward shift in convective regions as well as a southward expansion in Arctic ice. On the other hand, if the strength of the NAC were to increase, then it will cause heat transport farther north and a consequent decrease in ice cover (Aagaard and Carmack, 1994).

Estimates of the average Atlantic water inflow into the Barents Sea vary by a factor of two, ranging from less than 3 Sv to more than 5 Sv (Simonsen and Haugan, 1996). Reported values of the northward volume transport of Atlantic water through the Fram Strait with the West Spitsbergen Current (WSC) are also rather uncertain, varying from 2 to 6 Sv (Simonsen and Haugan, 1996). Two recent estimates indicate that the transport is in the range 2.9–3.7 Sv (Jónsson and Foldvik, 1992; Rudels et al., 1994). This means that the Barents Sea may receive about one-third of the total North Atlantic waters that flow into the GIN Sea over the Greenland–Scotland Ridge in the present-day situation (8 Sv; Hansen and Østerhus, 2000) and about half of the Atlantic water entering the Arctic Ocean. The Barents Sea thus, represents a significant heat and salt sink for the region. Furthermore, heat loss and brine rejection during winter leads to an increase in the density of the Atlantic waters in the Barents Sea. This modified Atlantic Water enters the Arctic Ocean from the Barents Sea partly through the opening between Novaya Zemlya and Franz Josef Land but mostly via the Kara Sea (Pfirman et al., 1994) (Fig. 1). The Barents Sea, therefore, acts as a mediator for the formation of dense water in the region.

Outflow of cold, dense bottom waters formed in the Barents Sea back into the GIN Sea takes place in the northern parts of the Bear Island Trough (Swift, 1986; Midttun and Loeng, 1987; Blindheim, 1989; Midttun, 1989) and through Storfjorden (Quadfasel et al., 1988). The effect of Barents Sea inputs on GIN Sea water masses and hence the WSC is not clear. But, if these inputs, including the export of sea-ice, are considered to modify the heat and salt content of the WSC, then the Barents Sea, besides contributing directly to the Arctic Ocean, also has an important indirect effect on the water masses of the Arctic Ocean (Hopkins, 1991).

In view of the role of the Barents Sea in the present-day ocean circulation pattern and based on some initial estimates, it is suggested that the late Cenozoic elevation changes in the Barents Sea could have played a key role in the evolution of the Polar North Atlantic palaeoclimate.

2. The Barents Sea

2.1. Location and sequence stratigraphy

The Barents Sea today is a shallow epicontinental sea with an average water depth of around 230 m and an area of about 1.2×10^6 km^2 (Fig. 1). It is bound in the north and west by Tertiary rift and shear margins (e.g., Faleide et al., 1993). The Novaya Zemlya region forms the eastern boundary whereas the Norwegian coast and the Kola Peninsula mark the southern boundary (Fig. 1). The bathymetry is characterised by banks and troughs.

The western Svalbard–Barents Sea Margin is characterised by large accumulations of sediments on the continental slope, believed to have resulted from late Cenozoic glaciations (e.g., Solheim et al., 1998). Seven regional seismic reflectors have been identified along this margin (Faleide et al., 1996) dividing the glacial sediments into six sequences (Fig. 2). The ages assigned to these reflectors (Table 1) follow Channell et al. (1999) and are based on palaeomagnetic data from Ocean Drilling Program (ODP) Site 986 (Fig. 1) with support from biostratigraphy (Eidvin and Nagy, 1999). The age estimates assume that the sequence boundaries i.e., reflectors R1–R7, represent time lines. Main sediment accumulations are found off Storfjorden and Bear Island troughs.

2.2. Modelling late Cenozoic elevation changes in the Barents Sea

At least two significant phases of uplift and erosion in the northern North Atlantic region are known to have occurred during the Cenozoic: one during late Palaeogene and the second around the Quaternary. The first event is attributed to the emplacement of magma from the Iceland plume in and below the crust while isostacy associated with glaciations is believed to have been important in the second event (Japsen and Chalmers, 2000). Whether or not glacio-isostacy was the only mechanism responsible for the late Cenozoic elevation changes is open to discussion. In the Barents Sea region,

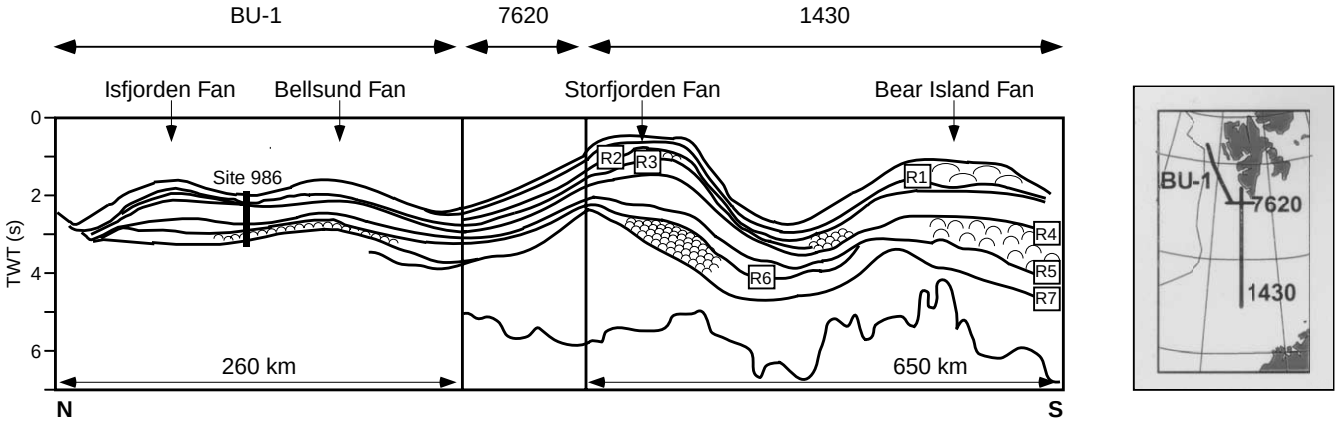

Fig. 2. A cartoon showing the seismic stratigraphy of the Svalbard–Barents Sea Margin (modified from Solheim et al., 1998).

Table 1
Estimates used for calculating elevation changes in
a) the Storfjorden drainage basin

Interval	Age (Ma)	Sed. Vol. (km^3) depositional	Sed. Vol. (cm^3) depositional	DBD (g/cm^3) depositional	Sed. mass (g)	DBD (g/cm^3) drainage	Sed. Vol. (cm^3) drainage	Sed. thickness (m) drainage
R7-R6	2.3–1.6	3.40×10^4	3.4×10^{19}	1.9	6.6×10^{19}	2.2	3.0×10^{19}	432
R6-R5	1.6–1.4	2.24×10^4	2.2×10^{19}	1.7	3.8×10^{19}	2.2	1.7×10^{19}	249
R5-R4	1.4–1.0	2.04×10^4	2.0×10^{19}	1.6	3.2×10^{19}	2.6	1.2×10^{19}	181
R4-R3	1.0–0.8	1.02×10^4	1.0×10^{19}	1.4	1.5×10^{19}	2.6	5.6×10^{18}	82
R3-R2	0.8–0.5	8.60×10^3	8.6×10^{18}	1.4	1.2×10^{19}	2.7	4.3×10^{18}	62
R2-R1	0.5–0.2	8.60×10^3	8.6×10^{18}	1.3	1.1×10^{19}	2.7	4.0×10^{18}	59
R1-SF	0.2–	5.70×10^3	5.7×10^{18}	1.0	5.9×10^{18}	2.7	2.2×10^{18}	32

b) the Bear Island drainage basin. DBD = dry bulk density, SF = seafloor.

Interval	Age (Ma)	Sed. Vol. (km^3) depositional	Sed. Vol. (cm^3) depositional	DBD (g/cm^3) depositional	Sed. mass (g)	DBD (g/cm^3) drainage	Sed. Vol. (cm^3) drainage	Sed. thickness (m) drainage
R7-R6	2.3–1.6	7.70×10^4	7.7×10^{19}	1.8	1.4×10^{20}	1.8	7.7×10^{19}	134
R6-R5	1.6–1.4	2.20×10^4	2.2×10^{19}	1.8	4.0×10^{19}	1.8	2.2×10^{19}	38
R5-R4	1.4–1.0	6.40×10^4	6.4×10^{19}	1.6	1.0×10^{20}	2.0	5.1×10^{19}	89
R4-R3	1.0–0.8	3.20×10^4	3.2×10^{19}	1.6	5.1×10^{19}	2.0	2.6×10^{19}	44
R3-R2	0.8–0.5	4.80×10^4	4.8×10^{19}	1.6	7.7×10^{19}	2.0	3.8×10^{19}	67
R2-R1	0.5–0.2	4.80×10^4	4.8×10^{19}	1.6	7.7×10^{19}	2.0	3.8×10^{19}	67
R1-SF	0.2–	1.06×10^5	1.1×10^{20}	1.5	1.6×10^{20}	2.1	7.6×10^{19}	131

estimates of total Cenozoic erosion from different parts of the Barents Sea range from 500 to 3500 m with greatest erosion estimated for the northwestern parts (Hjelstuen et al., 1996; Rasmussen and Fjeldskaar, 1996; Dimakis et al., 1998). Two-thirds of this erosion took place during the late Cenozoic (Eidvin and Riis, 1989), the time of frequent glacial–interglacial changes in the region. Glacial erosion has thus been the most dominant even if not the only mechanism during the late Cenozoic. Consequently, in the current work, relief changes in the Barents Sea during the last $\sim$2.5 Myr are assumed to have taken place principally due to glacially driven exhumation.

For this work, a uniform grid consisting of 262 square cells, each measuring $50 \times 50\,km^2$, was laid over a bathymetric map (drawn at 20 m contour intervals) of the Barents Sea (Fig. 3). The grid covers areas interpreted as drainage areas for sedimentary deposits off Storfjorden (Hjelstuen et al., 1996) and Bear Island Trough (Fiedler and Faleide, 1996). The total area covered by the grid measures $655 \times 10^3\,km^2$. The contour value at the centre of each grid cell was used to define the average contour value for the whole cell and based on this, the present-day bathymetry of the presumed drainage area was reconstructed (Fig. 4). The bathymetry so constructed

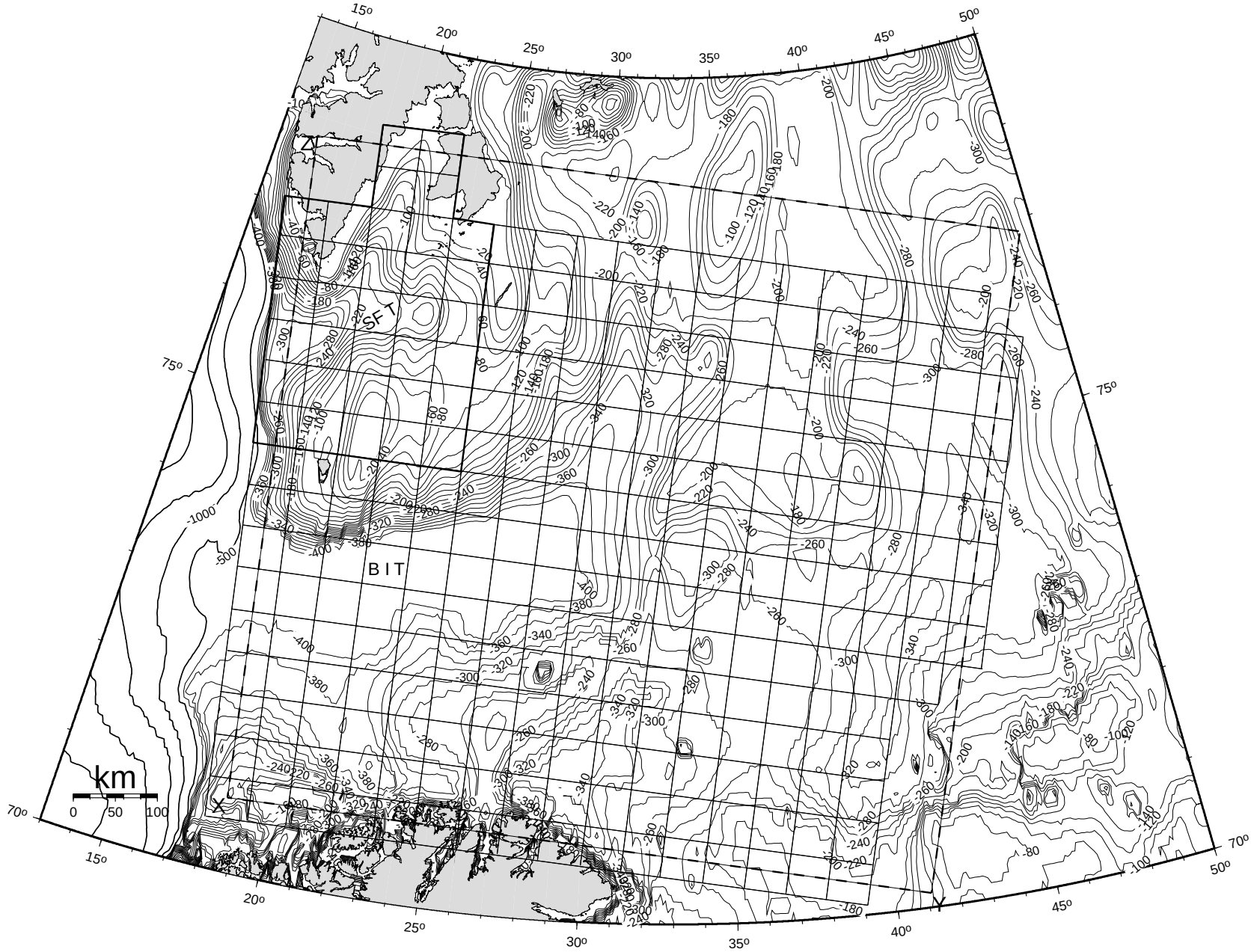

Fig. 3. The modelled area along with the overlain grid. The Storfjorden drainage area is outlined by heavier lines. The rectangle marked by the dashed line covers the area shown in Figs. 4 and 5. X, Y and Z are marked for orientation with Figs. 4 and 5.

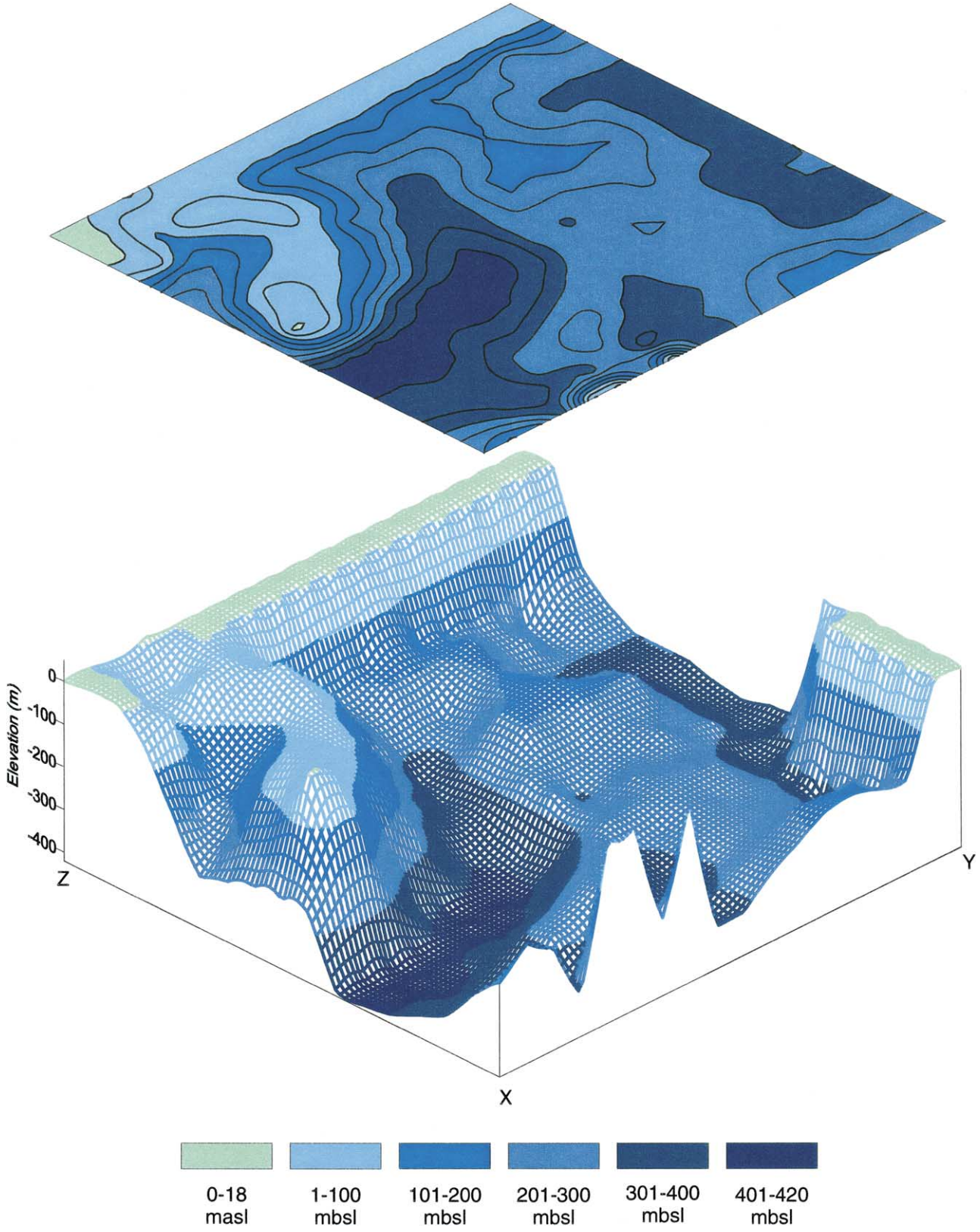

Fig. 4. Present-day bathymetry of the modelled area as constructed from the grid. Areas lying within the dashed rectangle but outside the grid at kept at zero elevation for the plot.

is a fair representation of the actual present-day bathymetry (cf. Figs. 3 and 4).

Hjelstuen (1993) and Hjelstuen et al. (1996) have constructed isopach maps for deposits off Storfjorden while Fiedler and Faleide (1996) have presented the same for the sedimentary wedge off Bear Island Trough. Based on these estimates and dating by Channell et al. (1999), sediment volumes for each time interval between R7 and R1 were calculated using linear interpolation for intervals where estimates are not available (Table 1).

An isostatic model by Dimakis et al. (1998) was used for relief simulations. The model is based on Airy's isostatic theory and response of the lithosphere to loading/unloading (deposition/erosion) is described by Airy isostatic equations. For a complete description of the equations and the way they are used, the reader is referred to the original paper by Dimakis et al. (1998).

Sediment volumes calculated for each of the seismic sequences in each of the two drainage basins (i.e., Storfjorden and Bear Island) were added together and divided by the respective drainage area. The resulting total sediment thickness for each basin was laid over its drainage area, as a slab of uniform thickness, to construct the relief of the Barents Sea at 2.3 Ma (R7 time) (Fig. 5a).

In the next step, the estimated sediment volume for the 2.3–1.6 Ma (R7–R6) interval, for each basin, was removed from the projected R7 relief and the model was run again. This procedure was repeated for each of the time intervals. Results for selected intervals are shown in Fig. 5.

The results show that the Barents Sea region was totally subaerial at 2.3 Ma and significant part of it became submarine after 1.0 Ma (Fig. 5).

The weaknesses associated with this modelling approach and sensitivity of the model output to input parameters have been discussed earlier in a similar modelling study (Butt et al., 2001). Sensitivity analyses were carried out to account for possible errors in estimates of drainage area, sediment densities, which in turn affect the estimates of sediment volume/thickness added or removed from the drainage area. While the elevations at different time intervals varied with changes in these input parameters (greater sediment thickness added = higher resulting topography, etc.) the timing of the transition from a primarily subaerial platform to a shelf sea was constrained to a relatively short time window of 200 kyr.

3. Exposed Barents Shelf and the oceanic regime in the Nordic Seas

Based on this work and earlier studies (e.g., Rasmussen and Fjeldskaar, 1996), a subaerially exposed Barents Sea during the Pliocene (i.e., before $\sim$2 Ma) is most likely. According to the model results, the Barents Sea dominantly became a shelf sea around 1 Ma (Fig. 1). It may thus be assumed that ocean circulation pattern similar to the present-day one is a phenomenon of the past ca. 1 Ma.

In addition to the elevation of the Barents Sea, there are several other parameters that need to be determined before an attempt can be made to ascertain the Pliocene oceanographic and climatic regimes. These include the palaeodepths of the openings that regulate exchange of water between the Arctic Ocean and the North Atlantic (Færoe–Shetland Ridge, Fram Strait, Denmark Strait) and the Arctic and the Pacific oceans (the Bering Strait), solar radiation balance, sea-level changes, palaeobathymetry, slope angles of the continental margins bordering the GIN Sea, etc.

As a first step, we have chosen to simulate the effect of an emergent Barents Shelf given the present-day oceanic and climatic forcing fields whose values are comparatively well known (e.g., Simonsen and Haugan, 1996; Hansen and Østerhus, 2000). Simulating the Pliocene climate with a global coupled ocean–sea ice–atmosphere model (Furevik et al., 2000) is planned as the next step.

3.1. The ocean model

MICOM is an ocean general circulation model that utilises surfaces of constant density (isopycnic surfaces) as the vertical coordinate (Bleck et al., 1992). The density of the upper layer is, however, free to evolve according to changes in the heat and freshwater fluxes caused by the thermodynamic forcing and mixing of the surface water. Prognostic variables in all of the layers are the horizontal velocity components, the layer thickness, and temperature. In addition, salinity is a prognostic variable in the upper surface layer, whereas salinity is diagnosed from the equation of state of seawater for all of the subsurface layers.

In the configuration used in this study (Drange, 1999), the reference pressure is set to zero, and the layer densities are expressed in σ_θ-units. There are 23 layers in the vertical, with σ_θ-values ranging from 24.05 to 28.11, and with a density spacing of 0.01 σ_θ-units for the most dense water masses. The layer densities have been chosen in order to describe the water mass characteristics of the major Atlantic–Arctic water masses.

The model domain covers the Atlantic Ocean from about 20°S and northwards, including the Arctic Ocean. The dynamic sea-ice model of Harder (1996) and the thermodynamic of Drange and Simonsen (1996) have been coupled to the ocean circulation model. The horizontal grid system is local orthogonal (Bentsen et al., 1999) with grid focus in the GIN Sea. The horizontal resolution in the GIN Sea varies from 55 to 65 km, whereas the grid spacing is about 250 km near the southern and northern model boundaries. The model

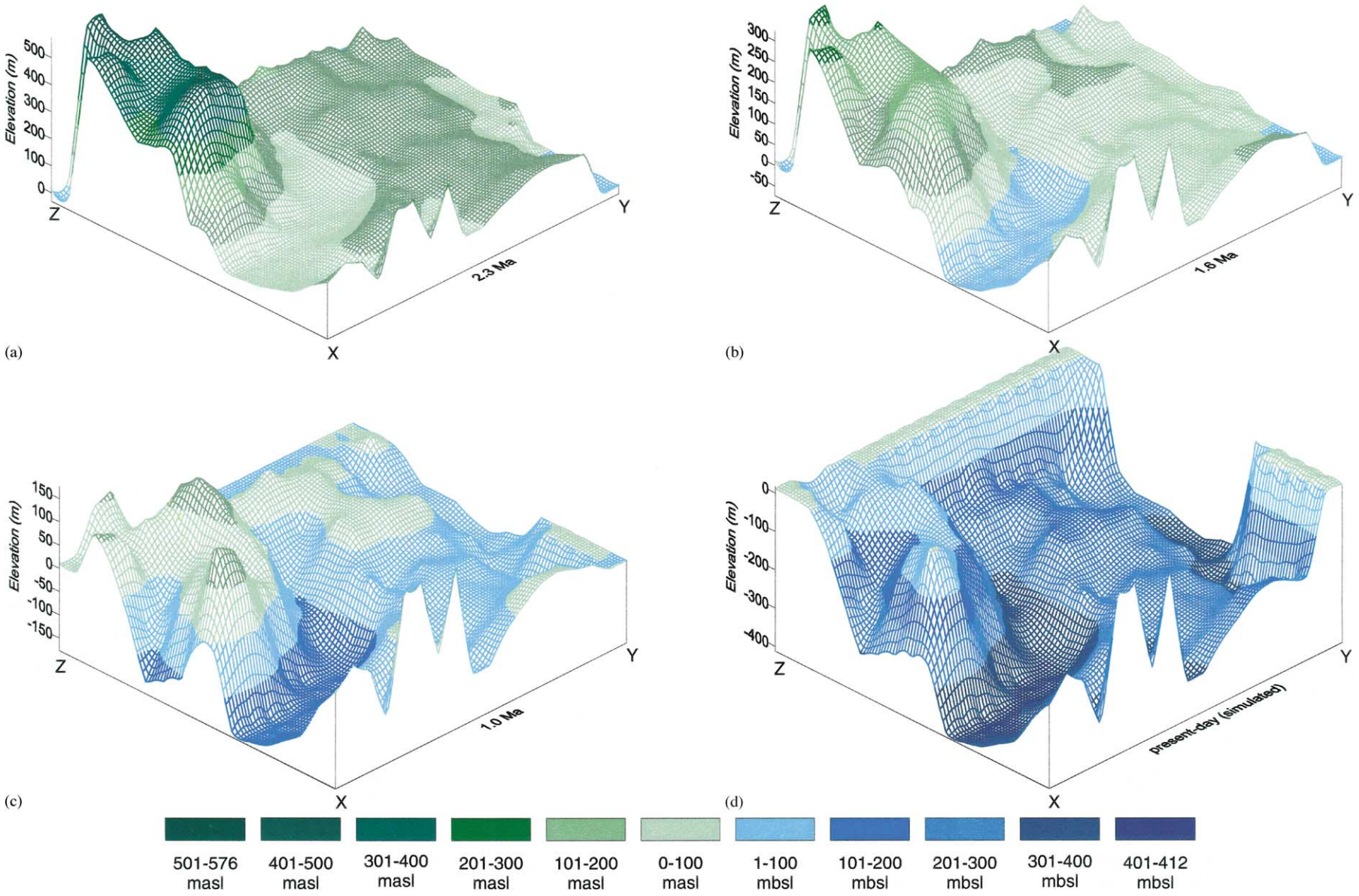

Fig. 5. Simulated topography of the Barents Sea at selected time intervals. Areas lying within the dashed rectangle but outside the grid at kept at zero elevation for the plots.

topography represents present-day conditions and for each model grid cell, the ocean depth has been calculated as the arithmetic mean of the 5-min resolution topography database ETOPO5 (NOAA, 1988).

The circulation model is initialised by observed hydrography (Levitus and Boyer, 1994; Levitus et al., 1994), and spun up from rest. As forcing fields, climatological monthly mean 10 m wind (ECMWF, 1988), 2 m surface air temperature (ECMWF, 1988; Simonsen and Haugan, 1996), cloudiness (Huschke, 1969; Oberhuber, 1988), precipitation (Legates and Willmott, 1990), and relative humidity (Maykut, 1978; Oberhuber, 1988) are used. The sea surface salinity (SSS) and temperature (SST) fields are relaxed towards observed monthly mean SSS and SST (Levitus et al., 1994; Levitus and Boyer, 1994) with a relaxation time scale of 1 month for a 100 m deep mixed layer (New et al., 1995). Temperature and salinity relaxations are switched off in the part of the Arctic Ocean where ice is present at maximum ice extent (typically occurring in March). The lateral boundaries at 20°S and south of the Bering Strait are treated as walls with vanishing water transports.

For the first 5 years, the ocean dynamics and thermodynamics evolve according to inconsistencies between the initial density structure and the applied surface forcing. After an integration time of about 10 years, the evolution of the simulated dynamics and thermodynamics approaches an annually repeated cycle. As an example, the net northward and southward transport of water through the Barents Opening between Svalbard and Northern Norway is displayed in Fig. 6. It follows from the figure that the net northward and southward volume transports are fairly stable year by year, and that there is a mean, northward transport of about 3.25 Sv and a southward transport of about 0.7 Sv through the opening. The simulated value of the inflow compares well with the Blindheim (1989) estimate of 3.1 Sv, whereas the outflow is underestimated compared to the value of 1.2 Sv given by Blindheim (1989).

Computations of the volume transported through some of the standard sections in the North Atlantic and the GIN Sea show that the major current systems are in general agreement with the large-scale circulation in the region (Nansen, 1906; Johannessen, 1986; Hopkins, 1991; Hansen and Østerhus, 2000). One exception is that the net southward transport of water through the Denmark Strait (about 2 Sv) is at the lower end of current estimates (e.g. Worthington, 1970; Hopkins, 1991). The reason for the somewhat weak flow through the Denmark Strait is not clear, but could be linked to insufficient horizontal grid resolution in the strait, or that the climatological surface wind-forcing fields are too weak. Comparison of model and satellite derived sea-ice concentrations in the Arctic shows that the simulated sea-ice field picks up many of the observed features (Lisæter et al., submitted). We, therefore, conclude that the ocean model applied in this study, despite problems like the weak southward transport through the Denmark Strait, describes the present-day circulation regime in a fairly realistic way.

The ocean model experiment reported here has been performed as a quasi-twin experiment, starting from year 20 of the spin-up integration. As a base case

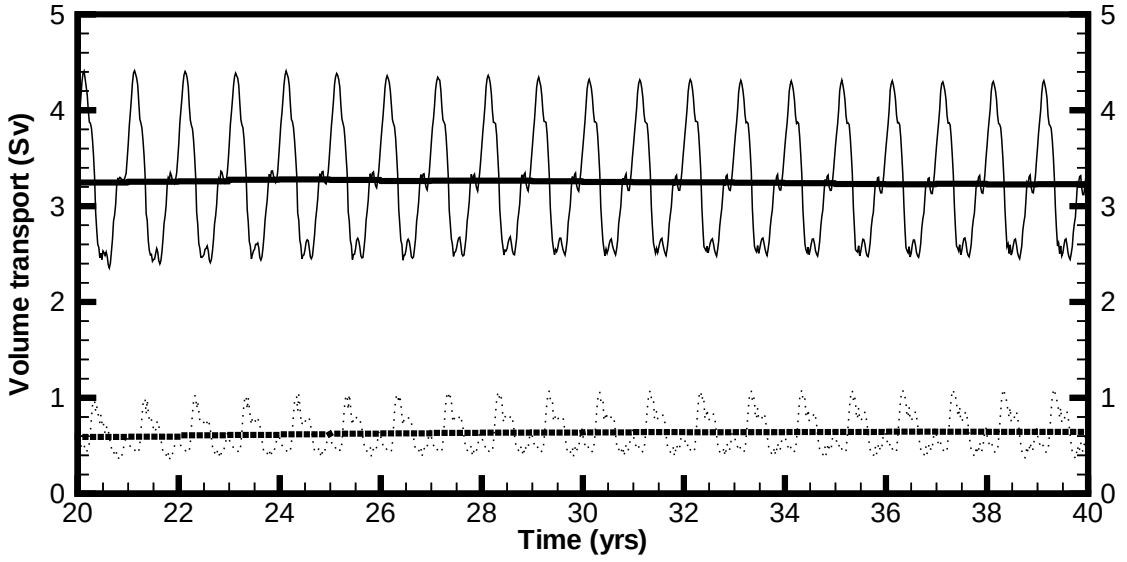

Fig. 6. Time series of the simulated northward (solid line) and southward volume transport (in Sv) through the Barents Opening for the years 20–40 of the control run.

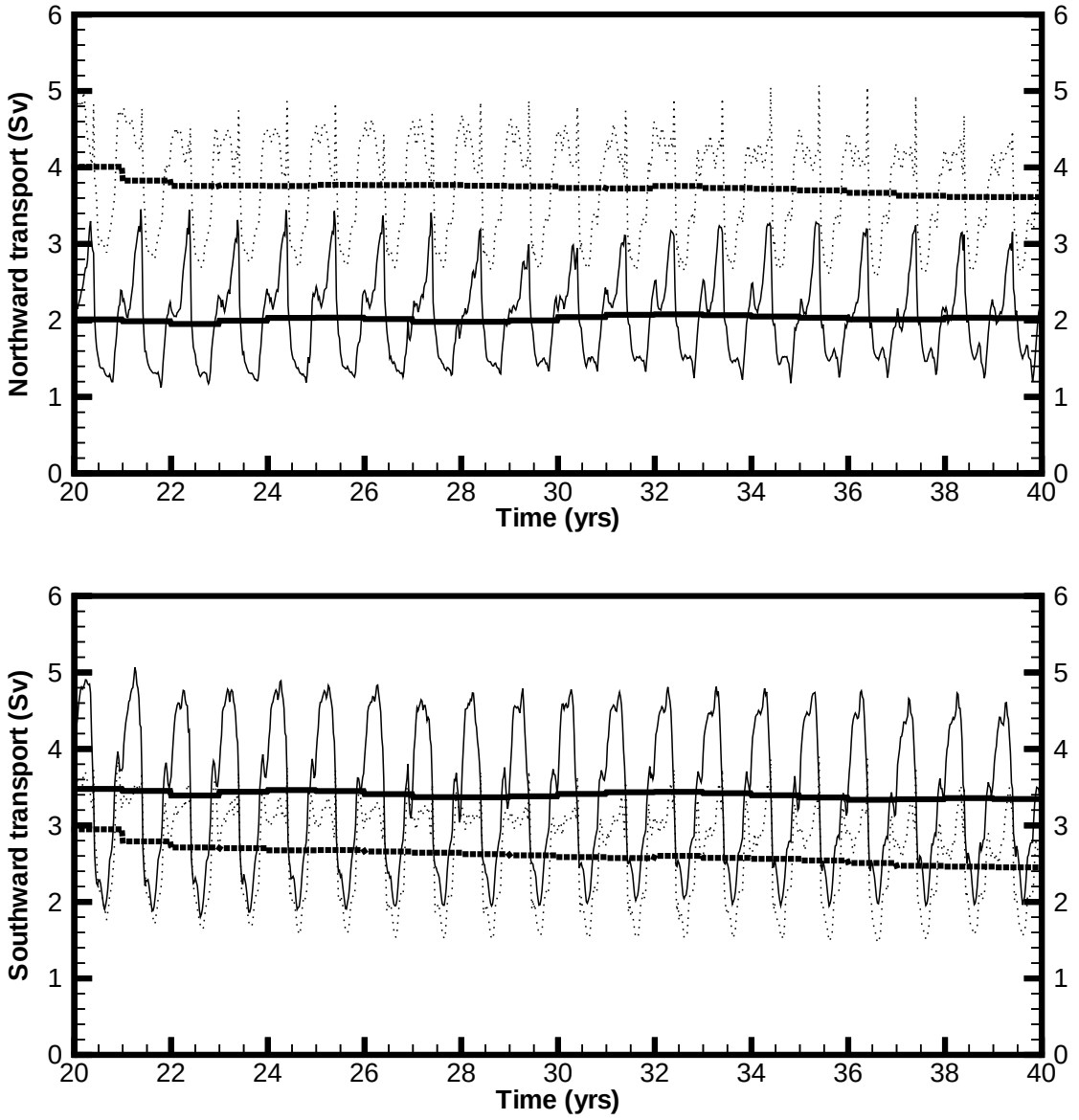

Fig. 7. Simulated northward (upper panel) and southward (lower panel) transports (in Sv) of water through the Fram Strait. Solid (dotted) lines represent open (closed) Barents Sea.

(or control) integration, the spin-up integration was continued for 20 years. Over this time period, negligible model drifts were observed in the simulated fields (Fig. 6). In the second integration, the Barents Sea region, bounded by Tromsø in Northern Norway and the islands, Spitsbergen, Franz Josef Land and Novaya Zemlya, was defined as land. The differences between the two simulations can then be attributed to the effect of closing the Barents Sea for water transports. In reality, the climate system consists of a series of non-linear coupling mechanisms between the atmosphere, the land surface and the ocean–sea ice environment, so the obtained results should only be viewed as a first attempt to examine possible climate effects of a closed Barents Sea (see Section 4).

3.2. Results

When the Barents Sea is closed i.e., subaerially exposed, the northward flowing Atlantic water is forced to follow the continental margin between northern Norway and Svalbard, leading to an intensification of the WSC. In the control simulation using the present-day scenario, about 2 Sv (Fig. 7) of the Atlantic water enters the Arctic Ocean with the WSC, whereas the remaining water recirculates in the strait and flows southward towards the GIN Sea. The situation with a closed Barents Sea is similar, but now the inflow almost doubles to a value of about 3.85 Sv (Fig. 7). As this water enters the Arctic Basin, it subducts under the cold and fresh (and consequently low density) surface water.

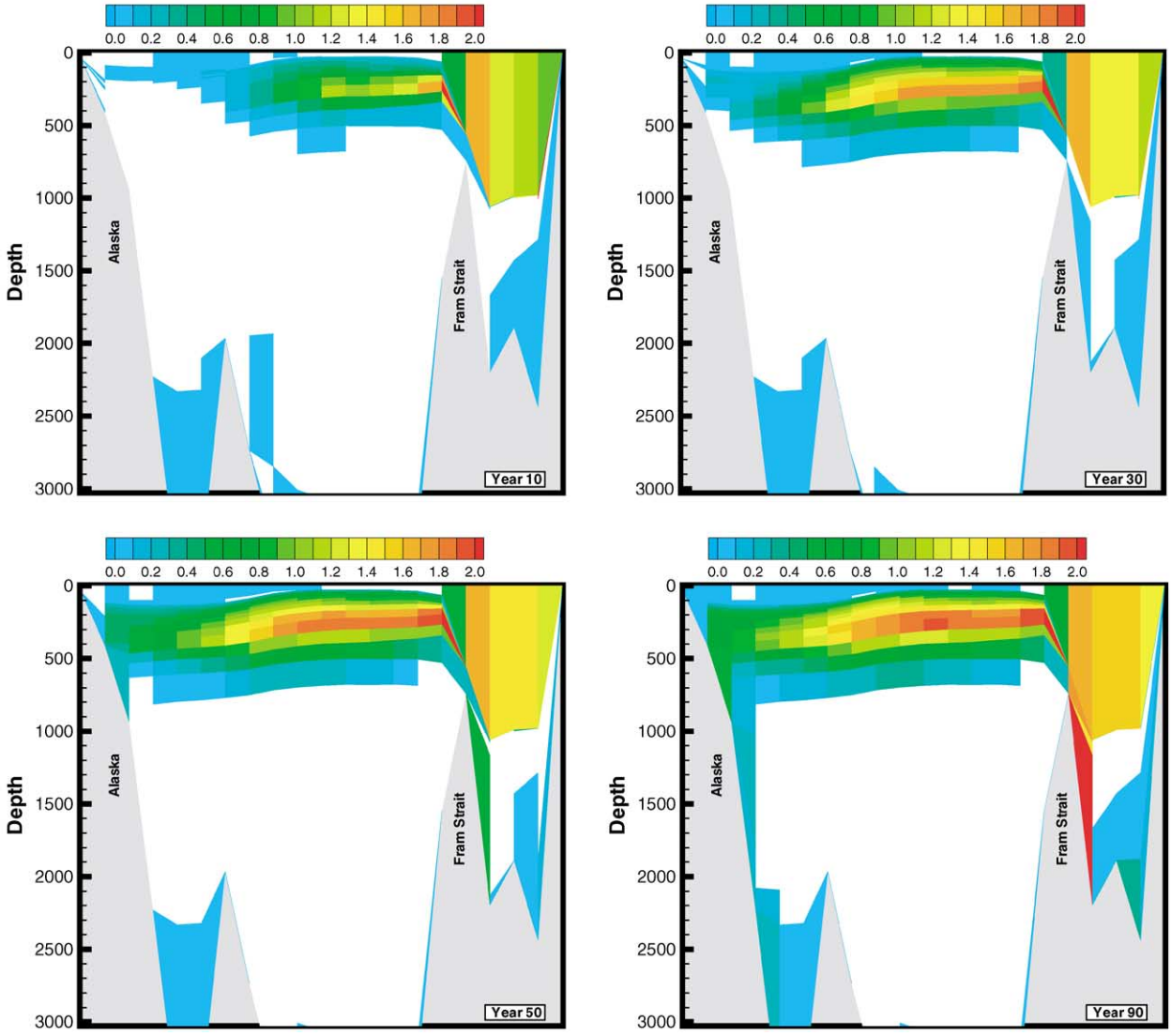

Fig. 8. Heating (K) of the waters in the Arctic Ocean along a vertical section through the Fram Strait towards Alaska in years 10, 30, 50 and 90 of the simulation with closed Barents Sea.

The increased transport of the Atlantic water into the Arctic Ocean leads to heating of the subsurface waters. In a vertical section through the Fram Strait and towards Alaska (Fig. 8), maximum heating of more than 1.5 K occurs at depths between 200 and 400 m. The heating of the subsurface waters increases with time. This is seen from Fig. 8, and is evident from the evolution of the vertical temperature profiles at a station north of Greenland and at the North Pole (Fig. 9). An extended integration period would lead to even stronger heating of the polar waters, but such experiments should be performed by global models without the artificial lateral boundaries applied in the regional model used here.

The horizontal distribution of the Atlantic water in the upper part of the Arctic Ocean is not uniform. Fig. 10 indicates strongest influence of this water, and consequently strongest heating, in a branch extending from the Fram Strait towards the Laptev Sea, and in a branch just north of Greenland. It is the core of the latter branch that is depicted in Fig. 8.

The simulated sea-ice evolves according to the heat balance at the top of the ice pack, and the horizontal and vertical inputs of heat into the upper ocean mixed layer. If ice is present and if the temperature of the surface mixed layer exceeds the melting temperature of sea-ice, ice is melted and the surface water temperature is reset to the melting temperature. This means that the temperature trace of the Atlantic water is removed from the surface water if ice melts. This, together with the subduction of the inflowing Atlantic water, is the reason for the near vanishing temperature change of the surface waters in Fig. 8.

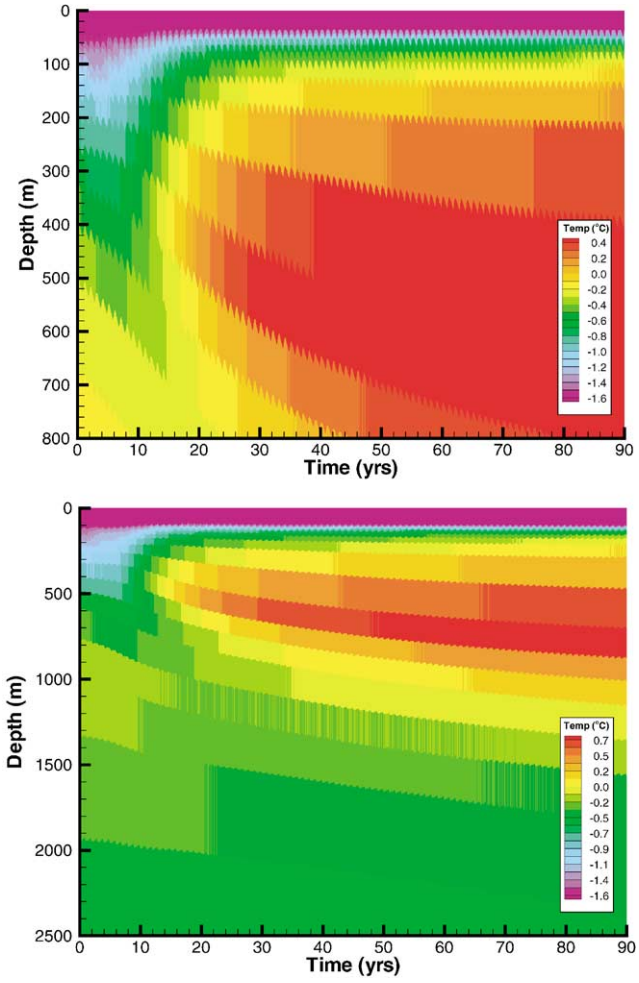

Fig. 9. Evolution of the vertical temperature (°C) profile at a location north of Greenland (upper panel: 85°N 118°W) and in the Central Arctic (lower panel: 86°N 13°W).

It appears from Fig. 10 that the upper 50–100 m of the central Beaufort Gyre, located in the Canada Basin, is only weakly affected by the warm Atlantic Water. However, the simulated sea-ice thickness indicates significant (about 1 m) melting of ice in the Beaufort Gyre after 90 years (Fig. 11). The reason for the melting is the persistent clockwise (anticyclonic) motion of the ice and surface waters in the Beaufort Gyre (e.g., Barry et al., 1993), leading to transport of Atlantic waters from the periphery towards the centre of the gyre, followed by melting of ice, resulting in a sea surface temperature equal to the melting temperature of ice.

On the contrary, if the presence of the Atlantic water was confined to the Arctic Ocean surface mixed layer, melting of the Polar Ice Cap would occur and the temperature of the surface layer could exceed the melting temperature of ice. In the present simulation, this is the case in and north of the Fram Strait and along the coast of East Greenland throughout the year. The open water regions, particularly during the cold winter and spring seasons, will feed large amounts of heat into the atmosphere. The climate effect of such heat sources is hard to assess without incorporating it into an atmosphere circulation model. As an indication of the amount of heat released from open waters in Polar regions, flux measurements from polynias in the Arctic Basin show a heat loss of more than $500\,\mathrm{Wm}^{-2}$ (Dethleff, 1994). The climate effect of ice-free waters in the Arctic Ocean may, therefore, be of importance for the local climate.

The modelled sea-ice response to the increased inflow of Atlantic water to the Arctic Basin is a general reduction in the thickness and extent of the ice. The only exception to this is a region north of Franz Josef Land where sea-ice accumulates due to pile-up of ice towards the new coastline. It follows from Fig. 11 that the reduction in ice thickness is larger in summer (represented by September) than in winter (March).

4. Discussion

The modelled elevation changes in the Barents Sea and their impact on ocean circulation in high northern latitudes are relevant for heat transport and mode of deep water formation in the Nordic Seas and on the extent of sea-ice formation in the Arctic Ocean.

The role of Arctic Ocean in regulating global climate, particularly, during the Cenozoic when the Earth's supercontinents were tectonically rearranged, has been a topic of intense debate for the past several decades. The theories have varied from scenarios where the Arctic Ocean is deemed to exert primary control on Northern Hemisphere climate through regulation of moisture supply from an ice-free Arctic (Ewing and Donn, 1956) or alternatively through the presence of an Antarctic-size ice cap regulating the sea-level fluctuations and δ^{18}O variations observed during the Pleistocene (Mercer, 1970; Broecker, 1975; Keigwin, 1982). In other instances, the Arctic Ocean is suggested to have initially merely responded to orbital forcing just like other parts of the Earth (e.g. Boyd et al., 1984) and then by a series of feedback mechanisms made a significant impact on maintaining world climate.

Likewise, the initial formation of the Arctic ice cover and its temporal variations have been a controversial topic and this issue is important because both the existence and extent of Arctic sea-ice cover are vital for processes such as heat exchange with the atmosphere and determining the site of deep-water formation which in turn can impact climate on regional/global scale. Clarke (1982) predicts a more or less consistent ice cover during the past 4 Ma and while conditions may have varied through glacial, deglacial and interglacial periods (Clarke and Morris, 1985), the Arctic Ocean is not believed to have been ice-free following the initial

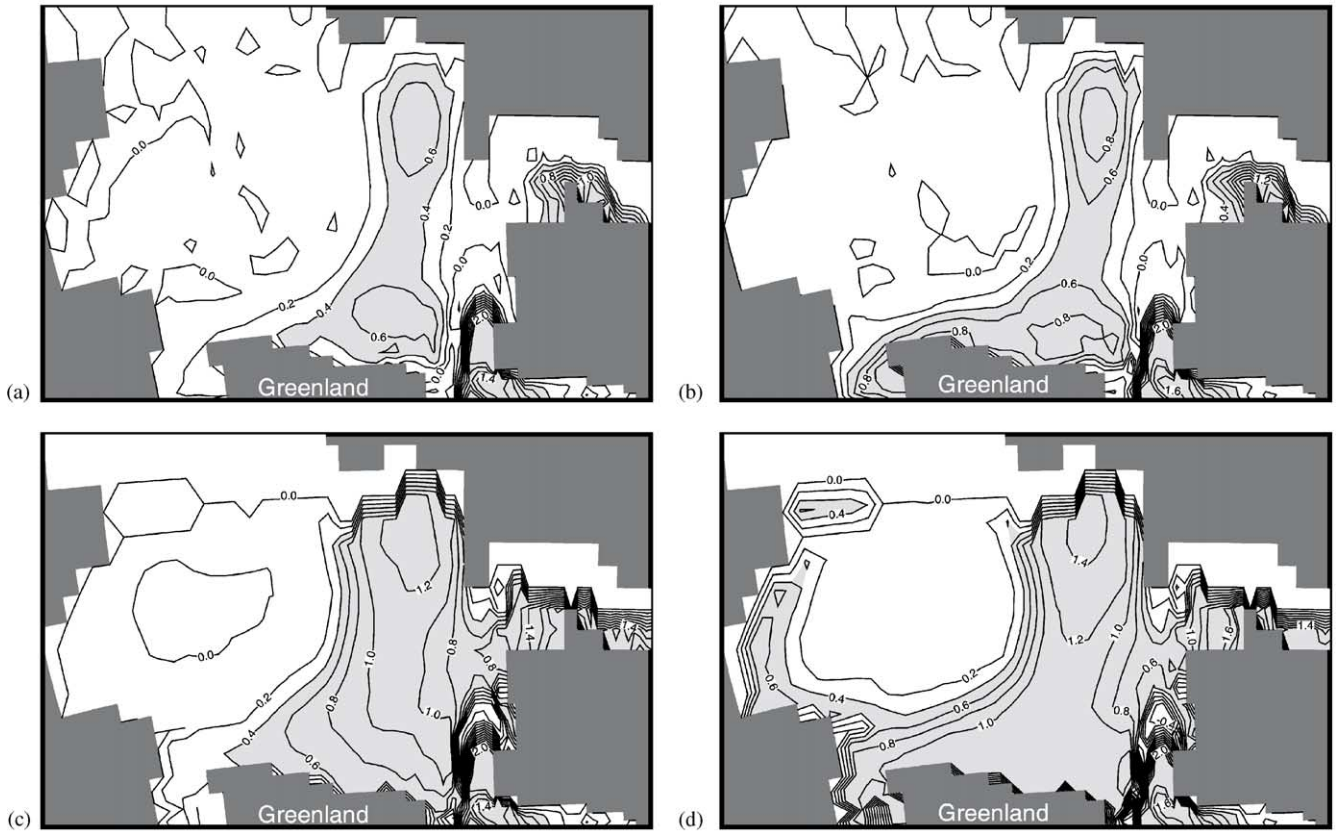

Fig. 10. Heating (K) of the waters in the Arctic Ocean at 50 m depth after (a) 20 years (b) 90 years, and at 100 m depth after (c) 20 years and (d) 90 years. Contour intervals 0.2 K, shaded area = heating > 0.4 K.

freezing (Untersteiner, 1969). On the other hand, the Pliocene–Holocene interval is suggested to have comprised of three main phases (Herman and Hopkins, 1980; Margolis and Herman, 1980; Worsely and Herman, 1980) including a cold but ice-free Arctic from ca 4.0–2.7 Ma, stratified saline and fresh water masses from 2.7–0.7 Ma and the 0.7 Ma-present interval characterised by the formation of first ice cover.

The major drawback in the interpretation of the Arctic data is lack of the reliable dating. Climatic fluctuations have been recognised in the Arctic sedimentary record based on the changes in texture, composition, structures, palaeontological and chemical content (e.g., Clarke et al., 1980; Morris et al., 1985; Mudie, 1985; Spielhagen et al., 1997; Jakobsson et al., 2000). Chronological models used have been based upon palaeomagnetic reversal stratigraphy (e.g., Schneider et al., 1996), and dating methods such as ^{10}Be (e.g., Aldahan et al., 1997), amino acids (Sejrup et al., 1984) or lithostratigraphy (e.g., Clarke et al., 1980) and interpolation between these and ^{14}C dating (Spielhagen et al., 1997). Clarke (1990) suggested that changes in the nature of the Arctic ice cover might be correlated with climatic events in the North Atlantic. However, even recent interpretations of data from the same area within the Arctic Ocean differ widely owing to different age estimates (e.g., Spielhagen et al., 1997; Jakobsson et al., 2000).

Furthermore, interpretations of the Plio-Pleistocene record from the Arctic Ocean and marginal areas around it show markedly different climatic regime than has been suggested from studies in the areas further to the south. There are reports of milder, sub-Arctic environments in NE Greenland around 2.45 Ma (Funder et al., 1985; Simonarson et al., 1998). Data from ODP Site 986 (off western Svalbard) do not bear any evidence of major glacial presence on Svalbard around this time (Smelror, 1999; Butt et al., 2000). On the other hand, intensification in the late Cenozoic Northern Hemisphere glaciations is dated to around 2.6 Ma (Jansen and Sjøholm, 1991; Tiedemann et al., 1994; Shackleton et al., 1995) whereby major ice sheets are envisaged to have occupied large areas over

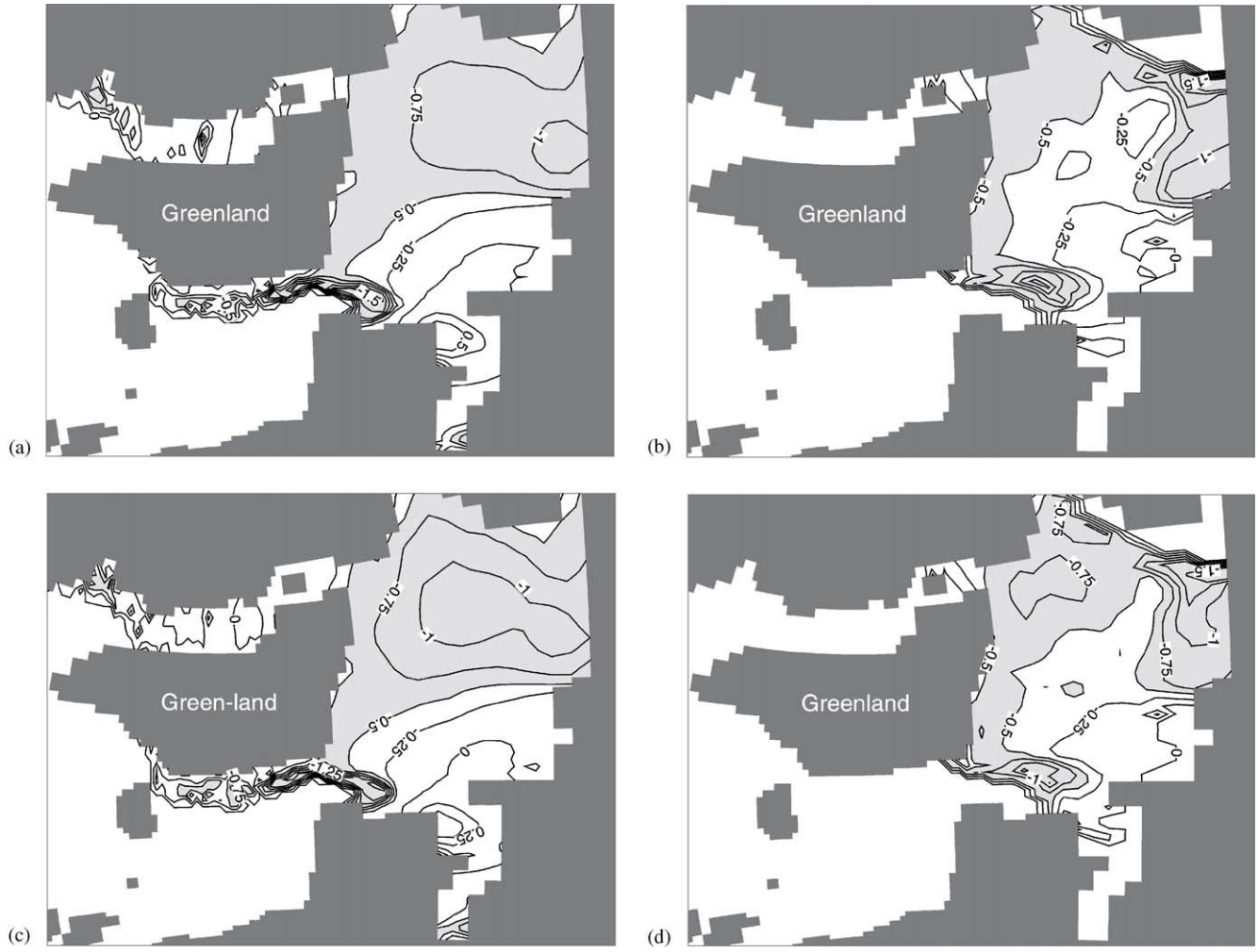

Fig. 11. Changes in the simulated ice thickness (m) after 20 years in (a) March (b) September, and after 90 years in (c) March and (d) September. Contour intervals: 0.25 K, shaded area = ice thickness reduction >0.5 m.

Greenland, Fennoscandia, Iceland, Svalbard and the Barents Sea.

This work enables us to comment on some earlier observations made in the Arctic and sub-Arctic regions that in our view are significant for interpreting the Plio-Pleistocene Arctic Ocean.

The modelling results presented herein indicate increased water and heat transport through the Fram Strait under a subaerial Barents Sea scenario (Figs. 8 and 9). This leads to warming of Arctic waters along two distinct paths; one along North Greenland and the other towards the Laptev Sea (Fig. 10) causing a reduction in ice thickness (Fig. 11). The current results thus provide a mechanism for explaining the findings of Funder et al. (1985) who, based on fauna and flora indicative of forest tundra environments found preserved in Kap København Formation, NE Greenland, proposed high-energy, marine environments during late Pliocene which Simonarson et al. (1998) date to 2.45 Ma. Funder et al. (1985) ruled out the possibility of a continuous perennial ice cover since the middle Cenozoic as proposed by Clarke (1982) and the modelling results tend to support that (Fig. 11).

The oceanographic simulations cover a period of ca. 100 years with a subaerial Barents Sea. The effects on a longer timescales are unclear but these preliminary findings suggest a seasonal, if any, Arctic sea-ice cover under such a scenario.

Butt et al. (2000) proposed onset of major glaciations on Svalbard around 1.6 Ma based on the data from ODP Site 986 off western Svalbard. Fig. 5 shows the development of the Bear Island Trough at this time allowing for water intake into the Barents Sea region. In theory, this would cause a reduction the strength of the WSC flowing towards the Fram Strait and at the same time provide a moisture source for inner parts of the Barents Shelf. Major parts of the Barents Sea are seen to become submarine around 1 Ma and a major shift in Northern Hemisphere

glaciations, the Mid-Pleistocene Revolution, is dated to around 0.9 Ma (Berger and Jansen, 1994). There is thus room to speculate that late Cenozoic elevation changes in the Barents Sea may have played an important role in the palaeoclimatic evolution of the Polar North Atlantic region.

5. Concluding remarks

The modelling results presented here raise important issues regarding the late Cenozoic palaeoclimatic evolution in the high northern latitudes and highlight the potentially important role the elevation of the Barents Sea and temporal changes therein, may play in this regard. As mentioned earlier, the concept of a once subaerial Barents Sea is not new but it has not been incorporated into the palaeoclimatic reconstructions for the Northern Hemisphere. The Barents Sea covered with a major ice sheet has been discussed (e.g., Siegert and Dowdeswell, 1996) but not as a subaerial shelf.

Mullen and McNeil (1995), based on foraminiferal evidence from the central Arctic Ocean, indicate probable connection between the Arctic and North Atlantic oceans during Pliocene and suggest a cold but milder palaeoclimate in the Arctic Ocean during early Pliocene than that which existed during Pleistocene glacial intervals. Results from ODP Leg 151 similarly indicate at least periodic intrusions of warm Atlantic waters into the Fram Strait during Late Pliocene (Cronin and Whatley, 1996; Osterman, 1996; Spiegler, 1996).

There is thus enough evidence to suggest inflow of warm waters in the Arctic and lower Arctic around 2.3 Ma. An uplifted Barents Sea at this time is a possible explanation for these observed warmer conditions. As results of ocean modelling indicate, such a scenario is likely to promote heat transfer to the Arctic Ocean with a consequent reduction in ice cover. The climatic consequences of a reduced ice cover have not been incorporated in the current work. However, in view of the role of the existing polynias in the Arctic Ocean and their role in heat exchange with the atmosphere (Aagaard and Carmack, 1994), open water conditions will cause increased heat exchange with the atmosphere over the Arctic Ocean and may lead to local, and possibly large scale, changes in climate.

The results, nevertheless, can only be regarded as preliminary at this stage. Several important related issues remain unanswered. These include, but are not limited to, the palaeodepths of the gateways, the atmospheric fields during late Pliocene (wind patterns, solar irradiance, etc.), the morphology of a subaerial Barents Shelf and its impact on atmospheric circulation and its drainage impact on the oceanic water masses, etc. Even the full climatic impacts under the present forcing fields cannot be understood without coupling ocean and sea-ice models with an atmospheric circulation model.

The final answers will, however, have to be provided by data from the Arctic Ocean itself. For this reason, it is important to come up with a reliable stratigraphy for the sedimentary record of the Arctic Ocean. Biostratigraphy holds the key in this regard. Lithostratigraphy and chemical properties of sediments are important but reliable dating is a pre-requisite for a valid palaeoclimatic reconstruction of the Arctic Ocean and its comparison with the record from the Nordic Seas and elsewhere. Only then can the impacts of various processes be understood.

Acknowledgements

The modelling of isostatic changes in the Barents Sea was carried out as part of a project funded by the Research Council of Norway (NFR) through Grant No. 116425/410. The ocean modelling work was supported by the G.C. Rieber Climate Institute at NERSC, and the Norwegian Research Council through the RegClim Project and Programme of Supercomputing. Dr. Wolfgang Berger and Dr. Ernst Maier-Reimer are gratefully acknowledged for their comments on an earlier draft of this paper. Two anonymous reviewers are thanked for critically reviewing the manuscript.

References

Aagaard, K., Carmack, E.C., 1994. The Arctic Ocean and climate: a perspective. In: Johannesen, O.M., Muench, R.D., Overland, J.E. (Eds.), The Polar Oceans and their Role in Shaping the Global Environment, Geophysical Monograph 85. American Geophysical Union, Washington, DC, pp. 5–20.

Aldahan, A.A., Shi Ning, Possnert, G., Backman, J., Bostrom, K., 1997. ^{10}Be records from sediments of the Arctic Ocean covering the past 350 ka. Marine Geology 144, 144–162.

Barry, R.G., Serreze, M.C., Maslanik, J.A., 1993. The Arctic sea-ice climate system: observations and modeling. Review of Geophysics 31 (4), 397–422.

Bentsen, M., Evensen, G., Drange, H., Jenkins, A.D., 1999. Coordinate trnasformation on a sphere using conformal mapping. Monthly Weather Reviews 123, 2733–2740.

Berger, W.H., Jansen, E., 1994. Mid-Pleistocene climate shift—the Nansen connection. In: Johannessen, O.M., Muench, R.D., Overland, J.E. (Eds.), The Polar Oceans and their Role in Shaping the Global Environment: The Nansen Centennial Volume, Geophysical Monograph 85. American Geophysical Union, Washington, DC, pp. 295–311.

Bleck, R., Rooth, C., Hu, D., Smith, L.T., 1992. Salinity-driven thermohaline transients in a wind- and thermohaline-forced isopycnic coordinate model of the North Atlantic. Journal of Physical Oceanography 22, 1486–1515.

Blindheim, J., 1989. Cascading of Barents Sea bottom water into the Norwegian Sea. Rapports et Proces-Verbaux des Reunions, Conseil International pour l'Exploration de la Mer 188, 49–58.

Boyd, R.F., Clark, D.L., Jones, G., Ruddiman, W.F., McIntyre, A., Pisias, N.G., 1984. Central Arctic Ocean response to Pleistocene Earth-orbital variations. Quaternary Research 22, 121–128.

Broecker, W.S., 1975. Floating glacial ice-caps in the Arctic Ocean. Science 218, 784–787.

Broecker, W.S., Peteet, D.M., Rind, D., 1985. Does the ocean–atmosphere system have more than one stable mode of operation? Nature 315, 21–26.

Butt, F.A., Elverhøi, A., Solheim, A., Forsberg, C.F., 2000. Deciphering late Cenozoic evolution of the western Svalbard Margin based of ODP Site 986 results. Marine Geology 169 (3-4), 373–390.

Butt, F.A., Elverhøi, A., Hjelstuen, B.O., Dimakis, P., Solheim, A., 2001. Modelling Late Cenozoic isostatic elevation changes in Storfjorden, NW Barents Sea: an indication of varying erosional regimes. Sedimentary Geology 143 (1-2), 71–89.

Channell, J.E.T., Smelror, M., Jansen, E., Higgins, S., Lehman, B., Eidvin, T., Solheim, A., 1999. Age models for glacial fan deposits off East Greenland and Svalbard (ODP Site 986 and Site 987). In: Raymo, M.E., Jansen, E., Blum, P., Herbert, T.D. (Eds.), Proceedings of the Ocean Drilling Program, Scientific Results 162. Texas A&M University, College Station, TX, pp. 149–166.

Clarke, D.L., 1982. Origin, nature and world climate effect of Arctic Ocean ice-cover. Nature 300, 321–325.

Clarke, D.L., 1990. Arctic Ocean ice cover: geologic history and climatic significance. In: Grantz, A., Johnson, L., Sweeney, J.F. (Eds.), The Arctic Ocean Region, The Geology of North America, Volume L. The Geological Society of America, Boulder, CO, pp. 53–62.

Clarke, D.L., Morris, T.H., 1985. Arctic Ocean sediment texture and the Pleistocene climate cycle. Geological Society of America Abstracts with Programs 17, 547.

Clarke, D.L., Whitman, R.R., Morgan, K.A., Mackey, S.D., 1980. Stratigraphy and glacial–marine sediments of the Amerasian Basin, central Arctic Ocean. Geological Society of America Special Paper 181, 57pp.

Cronin, T.M., Whatley, R., 1996. Ostracoda from Sites 910 and 911. In: Thiede, J., Myhre, A.M., Firth, J.V., Johnson, G.L., Ruddiman, W.F. (Eds.), Proceedings of the Ocean Drilling Program, Scientific Results 151. Texas A&M University, College Station, TX, pp. 197–201.

Dethleff, D., 1994. Polynyas as a possible source for energetic Bennett Island atmospheric plumes. In: Johannessen, O.M., Muench, R.D., Overland, J.E. (Eds.), The Polar Oceans and their Role in Shaping the Global Environment: The Nansen Centennial Volume, Geophysical Monograph 85. American Geophyiscal Union, Washington DC, pp. 475–483.

Dimakis, P., Braathen, B.I., Faleide, J.I., Elverhøi, A., Gudlaugsson, S.T., 1998. Cenozoic erosion and the preglacial uplift of the Svalbard–Barents Sea region. Tectonophysics 300, 311–327.

Drange, H., 1999. RegClim ocean modelling at NERSC. RegClim, regional climate development under global warming. General Technical Report 2, pp. 93–102.

Drange, H., Simonsen, K., 1996. Formulation of air–sea fluxes in the ESOP2 version of MICOM. Technical Report 125, Nansen Environmental and Remote Sensing Center, Bergen.

ECMWF, 1988. ECMWF forecast model. Physical parametrization. Research Manual 3, 2nd Edition, 1/88.

Eidvin, T., Nagy, J., 1999. Foraminiferal biostratigraphy of the Pliocene sequence at Site 986. In: Raymo, M.E., Jansen, E., Blum, P., Herbert, T.D. (Eds.), Proceedings of the Ocean Drilling Program, Scientific Results 162. Texas A&M University, College Station, TX, pp. 3–17.

Eidvin, T., Riis, F., 1989. Nye dateringer av de tre vestligste borehullene I Barentshavet. Resultater og konsekvenser for den tertiære hevingen. Norwegian Petroleum Directorate Contribution, 27 (in Norwegian).

Ewing, M., Donn, W.L., 1956. A theory of ice-ages. Science 128, 1061–1066.

Faleide, J.I., Vågnes, E., Gudlaugsson, S.T., 1993. Late Mesozoic–Cenozoic evolution of the south-western Barents Sea in a regional rift-shear tectonic setting. Marine and Petroleum Geology 10, 185–296.

Faleide, J.I., Solheim, A., Fiedler, A., Hjelstuen, B.O., Andersen, E.S., Vanneste, K., 1996. Late Cenozoic evolution of the western Barents Sea–Svalbard continental margin. Global and Planetary Change 12 (1-4), 53–74.

Fiedler, A., Faleide, J.I., 1996. Cenozoic sedimentation along the southwestern Barents Sea margin in relation to uplift and erosion of the shelf. Global and Planetary Change 12 (1–4), 75–93.

Funder, S., Abrahamsen, N., Bennike, O., Feyling-Hanssen, R.W., 1985. Forested arctic: evidence from North Greenland. Geology 13, 542–546.

Furevik, T., Kvamstø, N.G., Bentsen, M., Drange, H., Kindem, I.K.T, 2000. Preliminary results from a coupled atmosphere–ocean–sea ice model. In: Iversen, T., Høiskar, B.A.K. (Eds.), RegClim: Regional Climate Development Under Global Warming, Technical Report No. 4, Norwegian Institute for Air Research, pp. 121–133.

Hansen, B., Østerhus, S., 2000. North Atlantic–Nordic Seas exchanges. Progress in Oceanography 45, 109.

Harder, M., 1996. Dynamik, Rauhigkeit und Alter des Meereises in der Arktis. Ph.D. Thesis, Alfred-Wegner Institute of Polar and Marine Research, Germany, 124pp.

Herman, Y., Hopkins, D.M., 1980. Arctic Oceanic climate in Late Cenozoic time. Science 209, 557–562.

Hjelstuen, B.O., 1993. Late Cenozoic development of Storfjorden Fan based on re-processed multi-channel data. Unpublished Masters' Thesis, University of Oslo, 115pp. (in Norwegian).

Hjelstuen, B.O., Elverhøi, A., Faleide, J.I., 1996. Cenozoic erosion and sediment yield in the drainage area of the Storfjorden Fan. Global and Planetary Change 12 (1–4), 95–117.

Hopkins, T.S., 1991. The GIN Sea—a synthesis of its physical oceanography and literature review 1972–1985. Earth-Science Reviews 30, 175–318.

Huschke, R.E., 1969. Arctic cloud statistics from air calibrated surface weather observations. Memo. RM-5003-PR, Rand Corporation, Santa Monica, California.

IBCAO, 2000. Provisional map of the Arctic Ocean bathymetry. http://www.ngdc.noaa.gov/mgg/bathymetry/arctic/provisional-map.html

Jakobsson, M., Løvlie, R., Al-Hanbali, H., Arnold, E., Backman, J., Morth, M., 2000. Manganese and color cycles in Arctic Ocean sediments constrain Pleistocene chronology. Geology 28, 23–26.

Jansen, E., Sjøholm, J., 1991. Reconstruction of glaciation over the past 6 Ma based on Norwegian Sea records. Nature 349, 600–603.

Japsen, P., Chalmers, J.A., 2000. Neogene uplift and tectonics around the North Atlantic: overview. Global and Planetary Change 24, 165–173.

Johannessen, O.M., 1986. Brief overview of the physical oceanography. In: Hurdle, B.G. (Ed.), The Nordic Seas. Springer, Berlin, pp. 103–124.

Jónsson, S., Foldvik, A., 1992. The transport and circulation in Fram Strait. ICES C.M., C10, 10pp.

Keigwin, L.D., 1982. An Arctic Ocean ice-sheet in the Pleistocene? Nature 296, 808–809.

Legates, D.R., Willmott, C.J., 1990. Mean seasonal and spatial variability in guage-corrected, global precipitation. International Journal of Climatology 10, 111–127.

Levitus, S., Boyer, T.P., 1994. World Ocean Atlas 1994, Vol. 4: Temperature. NOAA Atlas NESDIS 4, Washington, DC, 117pp.

Levitus, S., Burgett, R., Boyer, T.P., 1994. World Ocean Atlas 1994, Vol. 3: Salinity. NOAA Atlas NESDIS 3, Washington, DC, 99pp.

Lisæter, K.A., Johannessen, O.M., Drange, H., Evensen, G., Sandven, S., Comparison of modeled and observed sea-ice concentration and thickness fields in the Arctic. Journal of Geophysical Research, submitted.

Margolis, S.V., Herman, Y., 1980. Northern hemisphere sea-ice and glacial development in late Cenozoic. Nature 286, 145–149.

Maykut, G.A., 1978. Energy exchange over young sea ice in the Central Arctic. Journal of Geophysical Research 83 (C7), 3646–3658.

Mercer, J.H., 1970. A former ice-sheet in the Arctic Ocean? Paleogeography, Palaeoclimatology, Paleoecology 8, 19–27.

Midttun, L., 1989. Climatic fluctuations in the Barents Sea. Rapports et Proces-Verbaux des Reunions, Conseil International pour l'Exploration de la Mer 188, 23–35.

Midttun, L., Loeng, H., 1987. Climatic variations in the Barents Sea. In: Loeng, H. (Ed.), The Effect of Oceanographic Distribution and Population Dynamics of Commercial Fish Stocks in the Barents Sea, Proceedings of the Third Soviet–Norwegian Symposium, Murmansk, pp. 13–28.

Morris, T.H., Clark, D.L., Blasco, S.M., 1985. Sediments of the Lomonosov Ridge and Makarov Basin: a Pleistocene stratigraphy for the North Pole. Geological Society of America Bulletin 96, 901–910.

Mudie, P.J., 1985. Palynology of CESAR cores, Alpha Ridge. Geological Survey of Canada Paper 84–22, pp. 59–99.

Mullen, M.W., McNeil, D.H., 1995. Biostratigraphic and paleoclimatic significance of a new Pliocene foraminiferal fauna from the central Arctic Ocean. Marine Paleontology 26 (1–4), 273–280.

Nansen, F., 1904. The bathymetrical features of the North-Polar Seas. Norwegian North Polar Expedition 1893–1896, Scientific Results 4(13), Christiania, 232pp.

Nansen, F., 1906. Northern waters. Captain Roald Asmudsen's oceanographic observations in the Arctic Seas in 1901 with a discussion of the origin of bottom waters in the Northern Seas. Videnskabs-selskabets skrifter 1, Mathematisk-Naturvidenskab Klasse 3, Christiania, 145pp.

Nansen, F., 1920. En ferd til Spitsbergen. Jacob Dywads, Kristiania, 279pp.

New, A.L., Bleck, R., Jia, Y., Marsh, R., Huddleston, M., Bernard, S., 1995. An isopycnic model study of the North Atlantic. Part 1: model experiment. Journal of Physical Oceanography 25, 2679–2711.

NOAA, 1988. Data Announcement 88-MGG-02, Digital relief of the surface of the Earth. NOAA, National Geophysical Data Center, Boulder, CO.

Oberhuber, J.M., 1988.The Budgets of Heat, Buoyancy and Turbulent Kinetic Energy at the Surface of the Global ocean. Max-Planck Institut fur Meteorologie, Hamburg, 15pp.

Osterman, L.E., 1996. Pliocene and Quaternary benthic foraminifers from Site 910, Yermak Plateau. In: Thiede, J., Myhre, A.M., Firth, J.V., Johnson, G.L., Ruddiman, W.F. (Eds.), Proceedings of the Ocean Drilling Program, Scientific Results 151. Texas A&M University, College Station, TX, pp. 187–195.

Pfirman, S.L., Bauch, D., Gammelsrød, T., 1994. The Northern Barents Sea: water mass distribution and modifications. In: Johannessen, O.M., Muench, R., Overland, J.E. (Eds.), The Polar Oceans and their Role in Shaping the Global Environment. Geophysical Monograph 85. American Geophysical Union, Washinton, DC, pp. 77–94.

Quadfasel, D., Rudels, B., Kurz, K., 1988. Outflow of dense water from a Svalbard fjord into the Fram Strait. Deep-Sea Resouces 35 (7), 1143–1150.

Rasmussen, E., Fjeldskaar, W., 1996. Quantification of the Pliocene–Pleistocene erosion of the Barents Sea from present-day bathymetry. Global and Planetary Change 12 (1–4), 119–133.

Rudels, B., Jones, E.P., Anderson, L.G., Kattner, G., 1994. On the intermediate depth waters of the Arctic Ocean. In: Johannessen, O.M., Muench, R.D., Overland, J.E. (Eds.), The Polar Oceans and their Role in Shaping the Global Environment. Geophysical Monograph 85. American Geophysical Union, Washington, DC, pp. 33–46.

Schneider, D.A., Backman, J., Curry, W.B., Possnert, G., 1996. Paleomagnetic constraints on sedimentation rates in eastern Arctic Ocean. Quaternary Research 46, 62–71.

Sejrup, H.P., Miller, G.H., Brigham-Grette, J., Løvlie, R., Hopkins, D., 1984. Amino acid epimerization implies rapid sedimentation rates in Arctic Ocean cores. Nature 310, 772–775.

Shackleton, N.J., Hall, M.A., Plate, D., 1995. Pliocene stable isotope stratigraphy of ODP Site 846. In: Mayer, L., Pisias, N., Janecek, T., et al. (Eds.), Proceedings of the Ocean Drilling Program, Scientific Results 138, Ocean Drilling Program. Texas A&M University, College Station, TX, pp. 337–355.

Siegert, M.J., Dowdeswell, J.A., 1996. Topographic control on the dynamics of the Svalbard–Barents Sea Ice Sheet. Global and Planetary Change 12 (1–4), 27–39.

Simonsen, K., Haugan, P.M., 1996. Heat budgets of the Arctic Mediterranean and sea surface heat flux parameterizations for the Nordic Seas. Journal of Geophysical Research 101, 6553–6576.

Simonarson, L.A., Petersen, K.S., Funder, S., 1998. Molluscan palaeontology of the Pliocene–Pleistocene Kap København Formation, North Greenland. Meddelelser om Grønland, Geoscience 36, 104pp.

Smelror, M., 1999. Pliocene–Pleistocene and redeposited dinoflagellate cysts from the western Svalbard Margin (Site 986): biostratigraphy, paleoenvironments and sediment provenance. In: Raymo, M.E., Jansen, E., Blum, P., Herbert, T.D. (Eds.), Proceedings of the Ocean Drilling Program, Scientific Results 162. Texas A&M University, College Station, Texas, pp. 83–97.

Solheim, A., Faleide, J.I., Andersen, E.S., Elverhøi, A., Forsberg, C.F., Vanneste, K., Uenzelmann-Neben, G., Channell, J.E.T., 1998. Late Cenozoic seismic stratigraphy and glacial geological development of the East Greenland and Svalbard–Barents Sea continental margins. Quaternary Science Reviews 17, 155–184.

Spiegler, D., 1996. Planktonic foraminifer Cenozoic biostratigraphy of the Arctic Ocean, Fram Strait (Sites 908–909), Yermak Plateau (Sites 910–912), and East Greenland Margin (Site 913). In: Thiede, J., Myhre, A.M., Firth, J.V., Johnson, G.L., Ruddiman, W.F. (Eds.), Proceedings of the Ocean Drilling Program, Scientific Results 151. Texas A&M University, College Station, TX, pp. 153–167.

Spielhagen, R.F., Bonani, G., Eisenhaur, A., Frank, M., Frederichs, T., Kassens, H., Kubik, P.W., Mangini, A., Nørgaard-Pedersen, N., Nowaczyk, N.R., Schaper, S., Stein, R., Thiede, J., Tiedemann, R., Wahsner, M., 1997. Arctic Ocean evidence for late Quaternary initiation of northern Eurasian ice sheets. Geology 25, 783–786.

Swift, J.H., 1986. Arctic waters. In: Hurdle, B.G. (Ed.), The Nordic Seas. Springer, New York, pp. 129–153.

Tiedemann, R., Sarnthein, M., Shackleton, N.J., 1994. Astronomic timescale for the Pliocene Atlantic d18O and dust flux records of ODP Site 659. Paleoceanography 9, 619–638.

Untersteiner, N., 1969. Sea ice and heat budget. Arctic 22, 195–199.

Worsely, T.R., Herman, Y., 1980. Episodic ice-free Arctic Ocean in Pliocene and Pleistocene times: calcareous nannofossil evidence. Science 210, 323–325.

Worthington, L.V., 1970. The Norwegian Sea as a Mediterranean Basin. Deep Sea Research 17, 77–84.